[Frontiers in Bioscience 10, 1368-1381 May 1, 2005]

ROLE OF SOME UNCONSERVED RESIDUES IN THE "C" REGION OF THE SKELETAL DHPR II-III LOOP

Angela F. Dulhunty, Yamuna Karunasekara, Suzanne M Curtis, Peta J. Harvey, Philip G. Board and Marco G. Casarotto

Division of Molecular Bioscience, JCSMR and Research School of Chemistry, ANU, Canberra, ACT 2601, Australia

TABLE OF CONTENTS

1. ABSTRACT

The actions of the recombinant skeletal dihydropyridine receptor II-III loop (*SDCL*), and the *C* region peptide (C_S) on native skeletal muscle ryanodine receptor Ca^{2+} release channel (RyR1) have been examined. Three non conserved residues in the "*C*" region of the skeletal DHPR II-III loop were replaced by the equivalent cardiac residues in $SDCL_{AFP\text{-}PTT}$ (A739P, F741T and P742T) and single substitutions made in $SDCL_{A\text{-}P}$, $SDCL_{F\text{-}T}$ and $SDCL_{P\text{-}T}$. Wild type *SDCL* as well as $SDCL_{F\text{-}T}$ and $SDCL_{P\text{-}T}$ activated RyR1 in lipid bilayers with high affinity (10 nM to 1 microM). Wild type *SDCL* at higher concentrations inhibited RyR1. In contrast, $SDCL_{AFP\text{-}PTT}$ and $SDCL_{A\text{-}P}$ inhibited the channels at ≥10 nM. The inhibitory actions of these two skeletal loop mutants were distinctly different from the cardiac II-III loop (*CDCL*) which, like the wild-type *SDCL*, activated channels. In contrast to the full loop, the triple A739P, F741T and P742T mutation in peptide C_S converted the peptides' function from skeletal-like to cardiac-like. The individual A739P mutation, but not F741T or P742T, reduced the functional efficacy of C_S. None of the mutations significantly altered the NMR-based secondary structure of the *C* residues in $SDCL_{AFP\text{-}PTT}$ or C_S. The C_S peptide and its mutants, like the cardiac C_C peptide, were all partially alpha helical at low temperatures. The results show that residue A739 is critical for the functional consequences of interactions between RyR1 and either the skeletal II-III loop or C_S, but that none of A739, F741 or P742 are critical determinants of the structure of the *C* region.

2. INTRODUCTION

The aim of this study was to examine interactions between the II-III loop of the skeletal dihydropyridine receptor (DHPR) L-type Ca^{2+} channel and skeletal ryanodine receptor (RyR1) channels. The work focuses on the effects of mutations in three key residues in the II-III loop on its structure and function. The DHPR, located in the surface/transverse-tubule membrane, communicates external electrical signals to the RyR Ca^{2+} release channel in the internal sarcoplasmic reticulum (SR) Ca^{2+} store. The RyR in cardiac muscle is activated during excitation-contraction (EC) coupling by a Ca^{2+} influx through the DHPR (1). In contrast in skeletal muscle, the RyR is thought to be activated by a protein-protein interaction with the DHPR. Thus it is of major importance to understand the nature of physical interactions between the skeletal DHPR and RyR. A sequence in the skeletal muscle II-III loop, between the 2nd and 3rd transmembrane repeats of the DHPR, is essential for skeletal type EC coupling (which is independent of Ca^{2+} influx) (2). Specific residues that are required for skeletal EC coupling have been identified in the "***C***" region (residues 724-760) of the skeletal II-III loop (3, 4) and are thus thought to be the focus of the physical interaction between the DHPR and RyR. The structure of these important skeletal "***C***" residues is either random coil at room temperature (5) or

Table 1. Synthetic peptides used in this study

Peptide C_S:	^{725}EFESNVNEVKDPYPSADFPGDDEEDEPEIPVSPRPRP^{769}
Peptide $C_{S\ AFP-PTT}$	^{725}EFESNVNEVKDPYPSPDTTGDDEEDEPEIPVSPRPRP^{769}
Peptide $C_{S\ A-P}$	^{725}EFESNVNEVKDPYPSPDFPGDDEEDEPEIPVSPRPRP^{769}
Peptide $C_{S\ F-T}$	^{725}EFESNVNEVKDPYPSADTPGDDEEDEPEIPVSPRPRP^{769}
Peptide $C_{S\ P-T}$	^{725}EFESNVNEVKDPYPSADFPGDDEEDEPEIPVSPRPRP^{769}
Peptide C_C:	^{725}DLQPNESEDKSPYPNPETTGEEDEEEPEMPVGPRPRP^{861}

partly helical at low temperatures (6), in marked contrast to the strongly α-helical structure of other regions of the skeletal loop (7, 8). The structure of the cardiac DHPR "***C***" region is not substantially different from that of the skeletal "***C***" region (6). The skeletal EC coupling domain has been further localized to residues in the 739–748 region (9). Residues 739, 741 and 742 are different in the cardiac and skeletal DHPR and substitution of the cardiac for skeletal residues interrupts skeletal EC coupling. It was predicted (a) that substitutions at positions 741 and 742 introduced alpha-helical structure into the ***C*** region of the II-III loop in conserved acidic residues located downstream from the mutations and (b) that the introduction of helical structure into these residues prevented the interaction between the DHPR and RyR (9). However, whole cell measurements of EC can be influenced by many factors other than the simple ability of two molecules to interact. Such factors include protein expression levels and micro targeting into tetrads exactly opposing RyRs at the molecular level. Molecular interactions between the DHPR and RyR cannot be directly studied in any available *in vivo* system. In this study we have looked at functional interactions between parts of the recombinant skeletal DHPR II-III loop (***SDCL***) or skeletal ***C*** region peptide ($\boldsymbol{C_S}$) with the RyR as well as the effect of the mutations on the interactions and on the structure of the "***C***" region.

Functional consequences of *in vitro* interactions between the DHPR and the RyR have been reported and are thought to reflect binding reactions that may contribute to protein-protein interactions in the intact cells. ***SDCL*** and $\boldsymbol{C_S}$, as well as the skeletal ***A*** peptide (residues 671-690), are high affinity activators of the skeletal RyR (1, 5, 10-15). We show here that introduction of cardiac residues into the three positions 739, 741 and 742 of ***SDCL*** ($\boldsymbol{SDCL_{AFP\text{-}PTT}}$ mutant) does not prevent its interaction with RyR1, but drastically alters the functional consequences of the interaction. The same changes are seen with a single substitution at residue 739, but not at residues 741 or 742. The actions of the $\boldsymbol{SDCL_{AFP\text{-}PTT}}$ and $\boldsymbol{SDCL_{A\text{-}P}}$ mutants were distinctly different from that of the cardiac II-III loop (***CDCL***). In contrast to the full loop, the triple mutation in the skeletal ***C*** peptide converted its activity from skeletal-like to cardiac-like. The results show that the activity of both the full skeletal II-III loop and the ***C*** peptide depend on residue A739. In contrast to the predictions made by Kugler *et al*. (9), we find that interactions between the proteins are maintained with the cardiac for skeletal substitutions in the 739 - 742 region and that there is no evidence for increased helical content as a result of the mutations. Our results do however indicate that at least one residue in this region is critical for the functional consequences of interactions between the RyR and DHPR.

3. MATERIALS AND METHODS

3.1. Materials

The following peptides were synthesised and purified (by the JCSMR Biomolecular Resource Facility) as previously described (7, 14, 16) (Table 1).

3.2. Expression of the DHPR II-III loop

The 391bp or 405bp cDNA fragments, respectively encoding the skeletal (***SDCL***) and cardiac (***CDCL***) DHPR II-III loop, were amplified by PCR and cloned in frame down stream of a poly-histidine tagged ubiquitin sequence in the plasmid pHUE (17). Mutations within the "***C*** " region of ***SDCL***, equivalent to those in the $\boldsymbol{C_S}$ peptides (above) were performed to yield $\boldsymbol{SDCL_{AFP\text{-}PTT}}$, $\boldsymbol{SDCL_{A\text{-}P}}$, $\boldsymbol{SDCL_{F\text{-}P}}$ and $\boldsymbol{SDCL_{P\text{-}T}}$ respectively, using the Quickchange XL-Site-directed mutagenesis kit (Stratagene). The normal and mutated constructs were checked by sequencing to exclude amplification errors. The plasmid was transferred into *E. coli* BL21 and expression of fusion protein induced by addition of 0.1 mM isopropyl-beta-D-thiogalactopyranoside to the culture media. The His-tagged protein was purified by chromatography on Ni-agarose (17, 18). Ubiquitin was removed from the N-terminal end of the II-III loop by digestion with a His-tagged ubiquitin-dependent protease (17). The ubiquitin protease and cleaved ubiquitin were removed by re-chromatography on Ni-agarose. The recombinant II-III loop, without additional residues, was further purified by preparative electrophoresis under native conditions using a Bio Rad model 491 prep cell. The sample was eluted in 25 mM Tris, 192 mM glycine pH 8.3. Uniformly ^{15}N labelled protein was produced by growing the expression strain in M9 minimal media with $^{15}NH_4Cl$ as the sole nitrogen source.

3.3. Single channel measurements

Recording solutions (7, 14, 16) were (mM) (*cis*): 230 $CsCH_3O_3S$, 20 mM CsCl, and 10 N-tris[hyroxymethyl]methyl-2-aminoethanesulfonic acid (TES, pH 7.4 with CsOH) and (*trans*): 230 $CsCH_3O_3S$, 20 CsCl, 1 $CaCl_2$ and 10 TES (pH 7.4). The *cis* Ca^{2+} concentration with 10^{-5} or 10^{-4} M Ca^{2+} was buffered using 1 mM BAPTA. The *cis* chamber was held at ground and the voltage of the *trans* chamber controlled. Bilayer potential, expressed as V_{cis} - V_{trans}, was changed between +40 and -40 mV every 30 s. Two minutes of activity was recorded under control conditions and after each addition of II-III loop or peptide.

3.4. Analysis of channel activity

Currents were analysed over one to two 30 s periods of continuous activity at +40 and –40 mV. Slow fluctuations in the baseline were corrected using an in house baseline-correction program (written by Dr DR Laver). Channel activity was measured either as "mean current" (average of all data points in a record) or as open probability (P_o), using a threshold analysis with the program *Channel 2,* (developed by PW Gage and M Smith, JCSMR). Measurements of mean current, performed on records from experiments containing 1 to 4 channels,

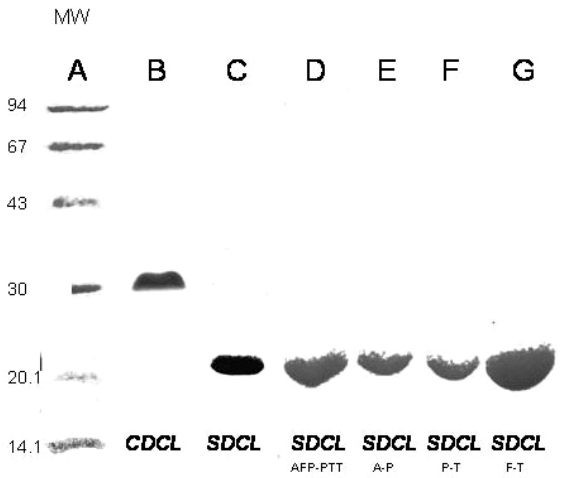

Figure 1. Expression of wild type ***CDCL, SDCL*** and ***SDCL*** mutant proteins**.** The purified recombinant proteins are shown on 12% denaturing polyacrylamide gels. Techniques for expression and purification of the proteins are given in the Methods section. Molecular weight markers are shown in the left lane (with corresponding weights), with ***CDCL*** in lane **B** (at ~30 kDa), ***SDCL*** in lane **C** (at ~21 kDa). The four ***SDCL*** mutants also run at ~21 kDa. $\boldsymbol{SDCL_{AFP\text{-}PTT}}$, $\boldsymbol{SDCL_{A\text{-}P}}$, $\boldsymbol{SDCL_{F\text{-}T}}$ and $\boldsymbol{SDCL_{P\text{-}T}}$ are shown in lanes **D**, **E**, **F** and **G** respectively.

included all channel activity from the smallest subconductance level to maximum openings. Open probability (P_O), mean open time (T_O) and mean closed time (T_C) measurements were restricted to records in which the opening of a single channel only was detected. This analysis does not detect openings that fall within the baseline noise. Threshold levels for channel opening and closing were set to exclude baseline noise, at ~20% of the maximum single channel conductance. Channel activity is expressed as relative P_O to include data in which P_O varied from ~0.01 to ~0.6 and data from bilayers containing more than one channel. Relative P_O was calculated either (a) from I't/I'c or (b) from P_Ot/P_Oc, where 't' denotes the parameter under test conditions and 'c' the control parameter. Since mean current divided by the maximum current approximates open probability, $I't/I'c \equiv P_Ot/P_Oc$.

3.5. Nuclear magnetic resonance (NMR) spectroscopy

The native and mutant $\boldsymbol{C_S}$ peptides were dissolved in 10% D_2O/90% H_2O to a final concentration of ~2 mM at pH 5.0. The samples for ***SDCL*** were prepared in 50 mM potassium phosphate buffer (pH 6.5) containing 10% D_2O, with a protein concentration of 1 mM in the presence of 200 mM KCl. All data was recorded at 5° C on a Varian Inova 600 MHz spectrometer equipped with a pentaprobe. In order to obtain resonance assignments one and two dimensional NMR spectroscopy was performed as described previously (7, 16). $^{15}N/^{1}H$ spectra were acquired using a sensitivity-enhanced ^{15}N-HSQC pulse sequence (19).

3.6. Statistics

The significance of differences between values was tested using a Students T-test, either 1 or 2 sided, for independent or paired data as appropriate or by the non parametric "Sign" test (20). Differences were considered significant when $P \leq 0.05$.

4. RESULTS

4.1. The recombinant native and mutant DHPR II-III loops

The recombinant 126 residue ***SDCL*** and 134 residue ***CDCL*****,** corresponding to the II-III loop of the $\alpha 1$ subunit of the skeletal and cardiac DHPR respectively, were expressed and purified (see Methods) and found to run on SDS-PAGE at the same molecular masses as those shown in (10), i.e. 30 kDA for ***CDCL*** and 21 kDa for ***SDCL*** (figure 1), which were higher than the calculated weights of 15.23 and 14.13 kDa repectively (6). The four mutant ***SDCL*** peptides appear on the SDS-PAGE gel at the same molecular masses as the wild type protein (figure 1).

4.2. Effects of wild type and mutant SDCL on the activity of the skeletal RyR1

The ***C*** peptides and recombinant II-III loops were added to the *cis* solution bathing the cytoplasmic side of native skeletal RyR1 channels. The channels were identified as RyRs by their Cs^+ conductance of ~250 pS and their block by 30 microM ruthenium red. The wild type ***SDCL*** activated the native channels at concentrations of 10 to 500 nM (figure 2), as previously reported with purified RyR1 channels (10). However in contrast to the purified channels, there was a decline in activity of the native channels with higher peptide concentrations (≥1 microM) indicating that the loop also had a low affinity inhibitory action. The relative P_O with 10 microM ***SDCL*** was significantly lower than that with 500 nM ***SDCL*** (figure 2C). Channel openings increased after perfusion of the *cis* chamber to dilute ***SDCL*** from 10 microM to ~3 nM (figure 2C), indicating a rapid reversal of the low affinity inhibitory action. Both the high affinity activation and low affinity inhibition by ***SDCL*** were similar at +40 and -40 mV (figure 2B), indicating that the effects of the recombinant II-III loop were voltage-independent. The current recordings in figure 2A reveal a substantial increase in channel open times and decrease in closed times during activation by ***SDCL*****.** These changes were observed in all channels and were significant in the average single channel data, with a 1.6-fold increase in open times and a 5-fold decrease in closed times (table 1).

In marked contrast to the wild-type ***SDCL***, addition of the triple mutant $\boldsymbol{SDCL_{AFP\text{-}PTT}}$ to the *cis* solution did not increase channel activity at either +40 or -40 mV (figure 3A & B). Indeed, there was a reversible inhibition which is apparent in the single channel records at ≥10 nM. The average decline in relative P_O was significant with 1 micoM $\boldsymbol{SDCL_{AFP\text{-}PTT}}$ (figure 3C). The reduced channel activity was due to a significant increase in the channel closed times, with essentially no change in open times (table 2). Perfusion of the mutant loop from the *cis* chamber was accompanied by a rapid increase in activity (figure 3C). The decline in activity, significant only at higher peptide concentrations, and its rapid recovery after washout were reminiscent of the low affinity inhibition seen

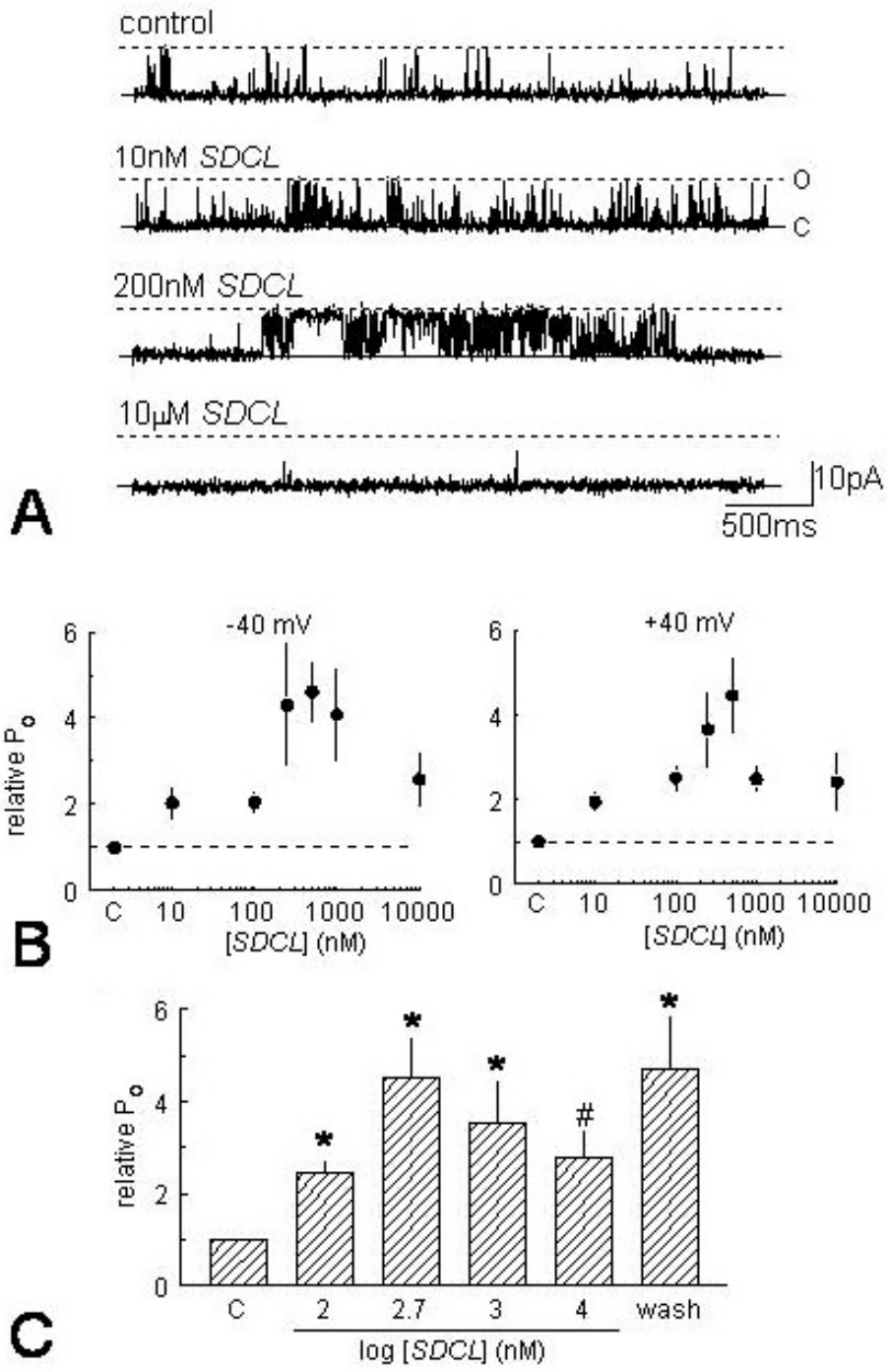

Figure 2. Wild type ***SDCL*** is a high affinity activator of native skeletal RyR1 channels and causes lower affinity inhibition. (**A**) shows current recordings from a single RyR1 channel at +40 mV. Channel opening is upward from the closed level (c, solid line) to the maximum single channel current (o, broken line). The channel is activated after 10 nM ***SDCL*** is added to its cytoplamic side and further activated when the [***SDCL***] is increased to 200 nM. There is a decrease in channel activity when [***SDCL***] is further increased to 10 microM. (**B**) – average relative open probability (P_O) as a function of [***SDCL***] at +40 mV (left) and -40 mV (right). Each point is the average of 4 to 22 experiments. The effect of the loop is the same at positive and negative potentials. (**C**) - average relative open probability (P_O) from 11 experiments in which the [***SDCL***] was increased from 10 nM to 10 microM and then perfused from the *cis* chamber. Average values include data obtained +40 mV and -40 mV. There is a reduction in channel activation at the higher ***SDCL*** concentrations and reversal of this inhibitory effect after loop washout. Asterisks in (C) indicate values that are significantly greater than the control. The hatch symbol indicates a significant decline in activity compared with the 500 μM ***SDCL*** value.

Table 2. Effects of various SDCL constructs on single RyR1 channel parameters.

	P_o reference	P_o *SDCL*	T_o reference	T_o *SDCL*	T_c reference	T_c *SDCL*
$\boldsymbol{SDCL}_{WT}$ N=7 (14)	0.039+/-0.013	0.112*+/-0.033	1.97+/-0.18	3.22*+/-0.77	277+/-81	53*+/-19
$\boldsymbol{SDCL}_{P\text{-}T}$ N=3 (6)	0.048+/-0.021	0.093+/-0.036	1.42+/-0.05	1.82*+/-0.18	169+/-87	56+/-22
$\boldsymbol{SDCL}_{F\text{-}T}$ N=1 (2)	0.017	0.055	2.04	2.56	491	114
$\boldsymbol{SDCL}_{AFP\text{-}PTT}$ N=8 (16)	0.031+/-0.01	0.015*+/-0.005	3.27+/-0.44	2.99+/-0.31	318+/-92	474*+/-122
$\boldsymbol{SDCL}_{A\text{-}P}$ N=5 (10)	0.143+/-0.047	0.051*+/-0.018	3.88+/-0.89	3.67+/-0.91	51.9+/-17.2	195*+/-78

Single channel parameters recorded before (reference) and after (***SDCL***) adding 1 microM of the wild type ($\boldsymbol{SDCL}_{WT}$) and mutant ***SDCL*** to bilayers in which a single RyR1 channel was active. N is the number of experiments. The number of observations (in parentheses) is double the number of experiments because data at +40 and -40 mV were included in the averages. Asterisks indicate significant changes induced by ***SDCL***.

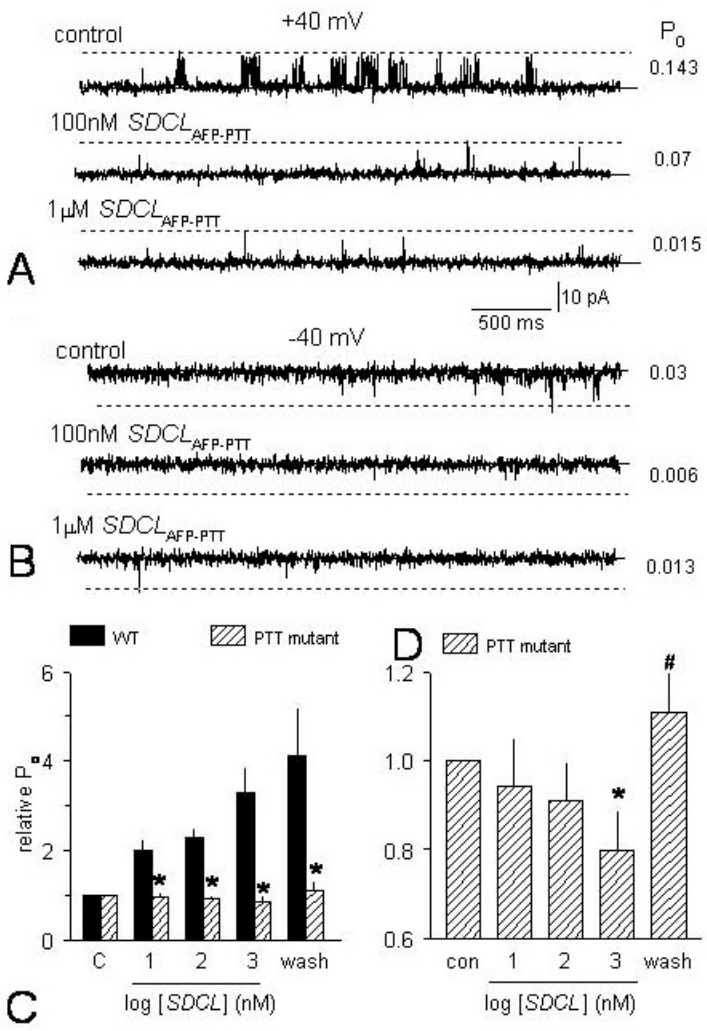

Figure 3. The triple mutant $\boldsymbol{SDCL}_{AFP\text{-}PTT}$ does not activate native RyR1, but does inhibit the channels. (**A**) & (**B**) show 3 s current recordings from a single RyR1 channel at +40 and -40 mV respectively. The channel opens from the closed level (c, solid line) to the maximum single channel current (o, broken line). The 1st trace in each panel shows control data, the 2nd trace after adding 100 nM $\boldsymbol{SDCL}_{AFP\text{-}PTT}$ to the *cis* chamber and the 3rd trace after increasing the concentration to 1 microM. The numbers to the right of each trace show P_O for a 30 s recording under each condition. Channel activity decreases as the peptide concentration is increased at both potentials. (**C**) – comparison of average relative open probability (P_O) (combined +40 and -40 mV data) for 11 experiments with wild type ***SDCL*** (filled bins – data from figure 2 included for comparison) and 8 experiments with $\boldsymbol{SDCL}_{AFP\text{-}PTT}$ (hatched bins)**.** The relative P_O with the mutant loop is significantly less than that with the wild-type loop during exposure and after washout, indicated by asterisks. (**D**) – average relative P_O with $\boldsymbol{SDCL}_{AFP\text{-}PTT}$ (hatched bins) displayed with an expanded vertical axis to display inhibition by the mutant loop. The asterisks in (**C**) indicate a significant difference between the mutant and wild-type data, while the asterisk in (**D**) indicates a significant decline from control with 1 microM $\boldsymbol{SDCL}_{AFP\text{-}PTT}$ and the cross-hatch indicates a significant recovery after washout of the loop.

with the native peptide. Thus the triple mutation appeared to abolish the high affinity activating effect of ***SDCL***, while leaving the low affinity inhibitory effect intact.

To determine whether all three cardiac residues were required for the functional difference between ***SDCL*** and $\boldsymbol{SDCL}_{\mathbf{AFP\text{-}PTT}}$, we substituted each of the residues individually. Substitution of the threonine for phenylalanine to position 741 ($\boldsymbol{SDCL}_{\mathbf{F\text{-}T}}$) or threonine for proline at position 742 ($\boldsymbol{SDCL}_{\mathbf{P\text{-}T}}$) had little effect on the activating ability of ***SDCL***. The records in figure 4A show that the single channel openings were more frequent and longer with $\boldsymbol{SDCL}_{\mathbf{F\text{-}T}}$, with an increase in P_O from 0.07 to 0.12. The mean current in the multiple channel experiment shown in figure 4B increased >3-fold after addition of $\boldsymbol{SDCL}_{\mathbf{P\text{-}T}}$, with one channel open in the bilayer under control conditions and 3 channels open with the mutant loop. As with the wild type protein, activation by the $\boldsymbol{SDCL}_{\mathbf{P\text{-}T}}$ was due to changes in both open and closed times, although in this case the increase in average open time alone was significant (table 1). Only one of 5 experiments with $\boldsymbol{SDCL}_{\mathbf{F\text{-}T}}$ was a single channel experiment and in that case the open times also increased and closed times fell (table 1). The changes in channel gating were similar with all three activating loop peptides, with the relative decrease in closed times being considerably greater than the relative increase in open times (table 1).

Unlike the F-T and P-T substitutions, substitution of a proline for the alanine at position 739 ($\boldsymbol{SDCL}_{\mathbf{A\text{-}P}}$) changed the effect of the loop on the RyR1 channels from activation to inhibition, in the same way as the triple mutation. The decline in channel activity was similar at both positive and negative potentials in the experiment in figure 5A&B and in 9 other experiments. The decline in average relative P_O was significant at all concentrations of $\boldsymbol{SDCL}_{\mathbf{P\text{-}T}}$ tested (10 nM to 1 micoM, figure 5C) and, like the inhibition with $\boldsymbol{SDCL}_{\mathbf{AFP\text{-}PTT}}$, was due to a significant increase in closed durations with essentially no change in the mean open time (table 1). Also similar to the action of $\boldsymbol{SDCL}_{\mathbf{AFP\text{-}PTT}}$, was the immediate increase in activity when the A-P mutant was washed out of the *cis* chamber in 11 of 14 cases (a significant increase according to the non-parametric sign test) (figure 5C). These results show that the A-P substitution alone was sufficient to remove activation and to unmask the full inhibitory action of ***SDCL***.

Since the AFP-PTT or A-P substitutions inserted cardiac residues into the skeletal sequence, it was of interest to see whether the effect of any of the mutant ***SDCL*** peptides mimicked the effect of the cardiac loop (***CDCL***) on RyR1. The results in figure 6A show that ***CDCL,*** like ***SDCL***, increased native RyR1 activity, although the increase in relative P_O was significantly less with ***CDCL***. Analysis of the one single channel experiment in this series showed that there was no change in open times and a 50% decline in closed times. This activation was also similar to, but less than, that with $\boldsymbol{SDCL}_{\mathbf{F\text{-}T}}$ or $\boldsymbol{SDCL}_{\mathbf{P\text{-}T}}$ and in marked contrast to the inhibitory effects of $\boldsymbol{SDCL}_{\mathbf{AFP\text{-}PTT}}$ and $\boldsymbol{SDCL}_{\mathbf{A\text{-}P}}$. Washout activation upon removal of ***CDCL*** was seen in only one of 4 observations, suggesting that inhibitory effect of ***CDCL*** may be weaker than that of ***SDCL*****.** Together, the results show that the mutations do not result in cardiac like loop activity. The F-T and P-T substitutions do not depress activation to the level seen with ***CDCL***, while the AFP-PTT and A-P substitutions produce mutants with activity unlike that seen with either the wild type skeletal and cardiac loops.

In conclusion, the A-P substitution in the skeletal loop changed the action of ***SDCL*** from excitatory to inhibitory, however the presence of the proline residue in ***CDCL*** did not render the cardiac loop inhibitory although ***CDCL*** produced significantly less activation of RyR1 than the skeletal loop. This results suggests that activation by the loop depends either (a) on binding more than one set of loop residues, so that the functional effects of "***C***" region binding are masked by effects of the binding of other regions in ***CDCL***, but not in ***SDCL*** or (b) more generally, that the functional effects of the proline residue are negated/reversed by other non-conserved regions/residues in ***CDCL***.

4.3. Effects of the mutant C_S peptides on skeletal RyR1

The effects of the same substitutions in the 36 residue peptide $\boldsymbol{C_S}$ (the skeletal ***C*** sequence, see Methods) were examined. The wildtype $\boldsymbol{C_S}$ activates skeletal RyRs at concentrations of 10 nM to 10 microM (5, 21). The triple mutant $\boldsymbol{C_{S\mathrm{AFP\text{-}PTT}}}$ also activated skeletal RyRs, although at a peptide concentration of 100 nM, the ~1.9-fold activation by the mutant peptide was significantly less than the ~4.4-fold activation by the wild-type peptide (Figure 6B). Indeed, activation by the triple mutant at 100 nM was not significantly different from the ~1.5-fold activation of skeletal RyRs produced by the cardiac ***C*** peptide, $\boldsymbol{C_C}$ (Figure 6B and (21)). Thus the activation of RyR1 by $\boldsymbol{C_{S\mathrm{AFP\text{-}PTT}}}$ appeared to be more like that of $\boldsymbol{C_C}$ than $\boldsymbol{C_S}$.

4.4. The mutant C_S peptide activates cardiac RyR2 channels

Cardiac channels provided a better functional probe for the different ***C*** peptides than RyR1 because the skeletal $\boldsymbol{C_S}$ peptide inhibits the channel, while the cardiac $\boldsymbol{C_C}$ peptide activates the channel, even though both peptides act at the same site on RyR2 (6). The results in figure 6C show that $\boldsymbol{C_{S\mathrm{AFP\text{-}PTT}}}$ strongly activated RyR2 in a very similar manner to peptide $\boldsymbol{C_C}$. Therefore the triple mutation also converted the action of the peptide on RyR2 from a skeletal-like to cardiac-like. Examination of the three individual $\boldsymbol{C_S}$ mutants showed that, in contrast to the full loop, none of the single substitutions were as effective as the triple substitution in changing the effect of the peptide from inhibition to activation. However, the ability of the A-P mutant to inhibit RyR2 was significantly less than that of the wildtype $\boldsymbol{C_S}$ or the P-T or F-T mutants (figure 6D). Although activation was not seen in the average $\boldsymbol{C_{S\mathrm{A\text{-}P}}}$ data, it was seen in 2 of the 5 experiments. In contrast to $\boldsymbol{C_{S\mathrm{A\text{-}P}}}$, all channels were inhibited in experiments in which $\boldsymbol{C_{S\mathrm{F\text{-}T}}}$ and $\boldsymbol{C_{S\mathrm{P\text{-}T}}}$ were added to the cytoplasmic solution. As with the full loop, the results again point to a critical role of an alanine at position 739 in determining the function of the ***C*** region of the skeletal II-III loop.

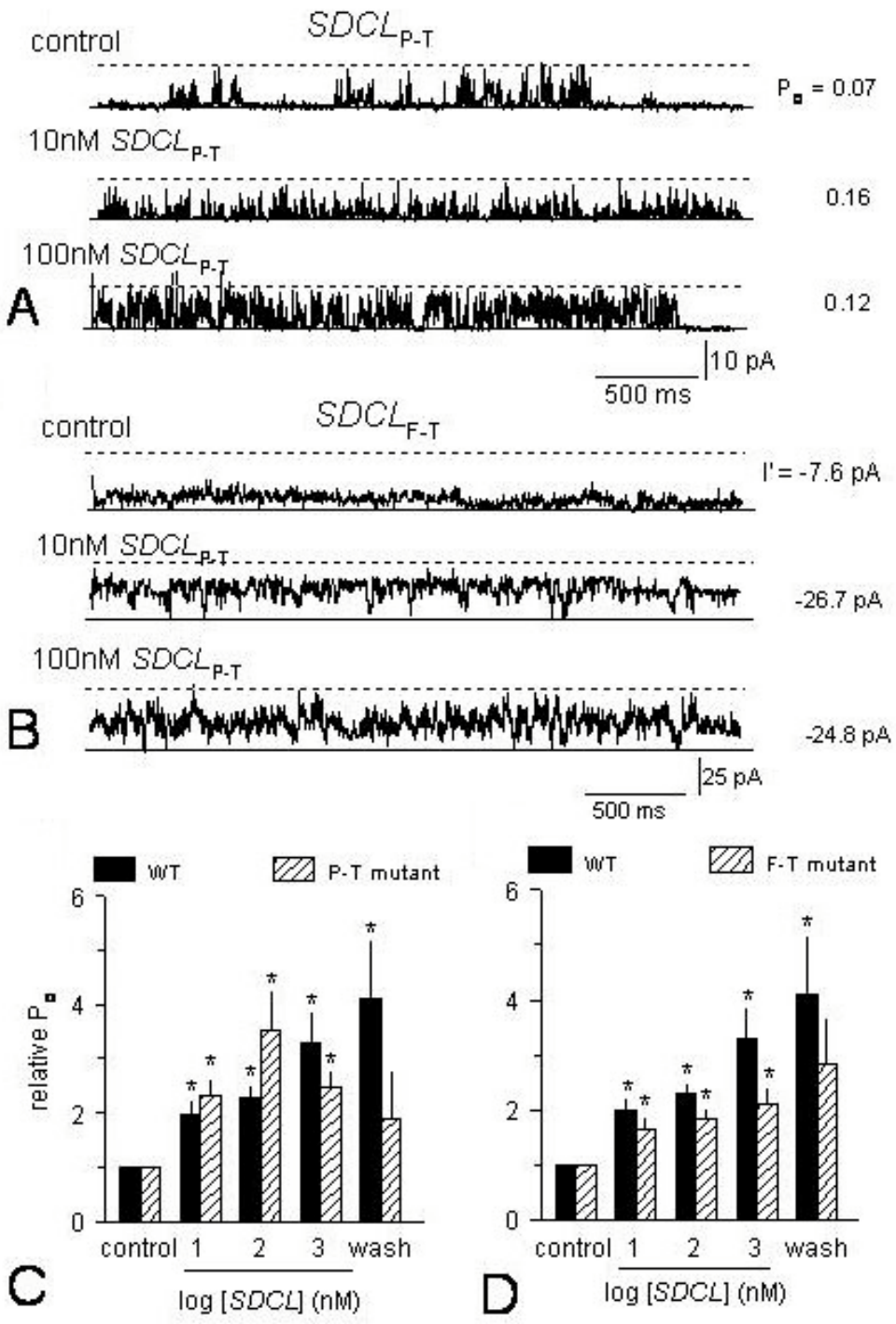

Figure 4. Individual mutants ***SDCL*$_{F-T}$** and ***SDCL*$_{P-T}$** activate RyR1 in a similar manner to the wild type ***SDCL***. (**A**) and (**B**) show 3 s current recordings +40 mV with channel opening from the closed level (c, solid line) to the maximum single channel current (o, broken line in (**A**)) or the maximum current for the 3 RyR channels (o_3, broken line in (**B**)). A single RyR channel exposed to ***SDCL*$_{F-T}$** is shown in (**A**) and current from a bilayer containing 3 channels after exposure to ***SDCL*$_{P-T}$** is shown in (**B**). The 1st trace in each panel shows control data, the 2nd trace after adding 10 nM loop to the *cis* chamber and the 3rd trace after increasing the concentration to 100 nM. The numbers to the right of each trace show P_O in (**A**) or I' (mean current) in (**B**) for a 30 s recording under each condition. (**C**) and (**D**) show average relative open probability (P_O) (combined +40 and -40 mV data) for 11 experiments with wild type ***SDCL*** (filled bins) and 5 experiments with ***SDCL*$_{F-T}$** (hatched bins in (**C**))and 10 experiments with ***SDCL*$_{P-T}$** (hatched bins in (**D**))**.** Data for the wild type ***SDCL*** (from figure 2) is included for comparison (filled bins). Asterisks in (**C**) and (**D**) indicate values that are significantly greater than control.

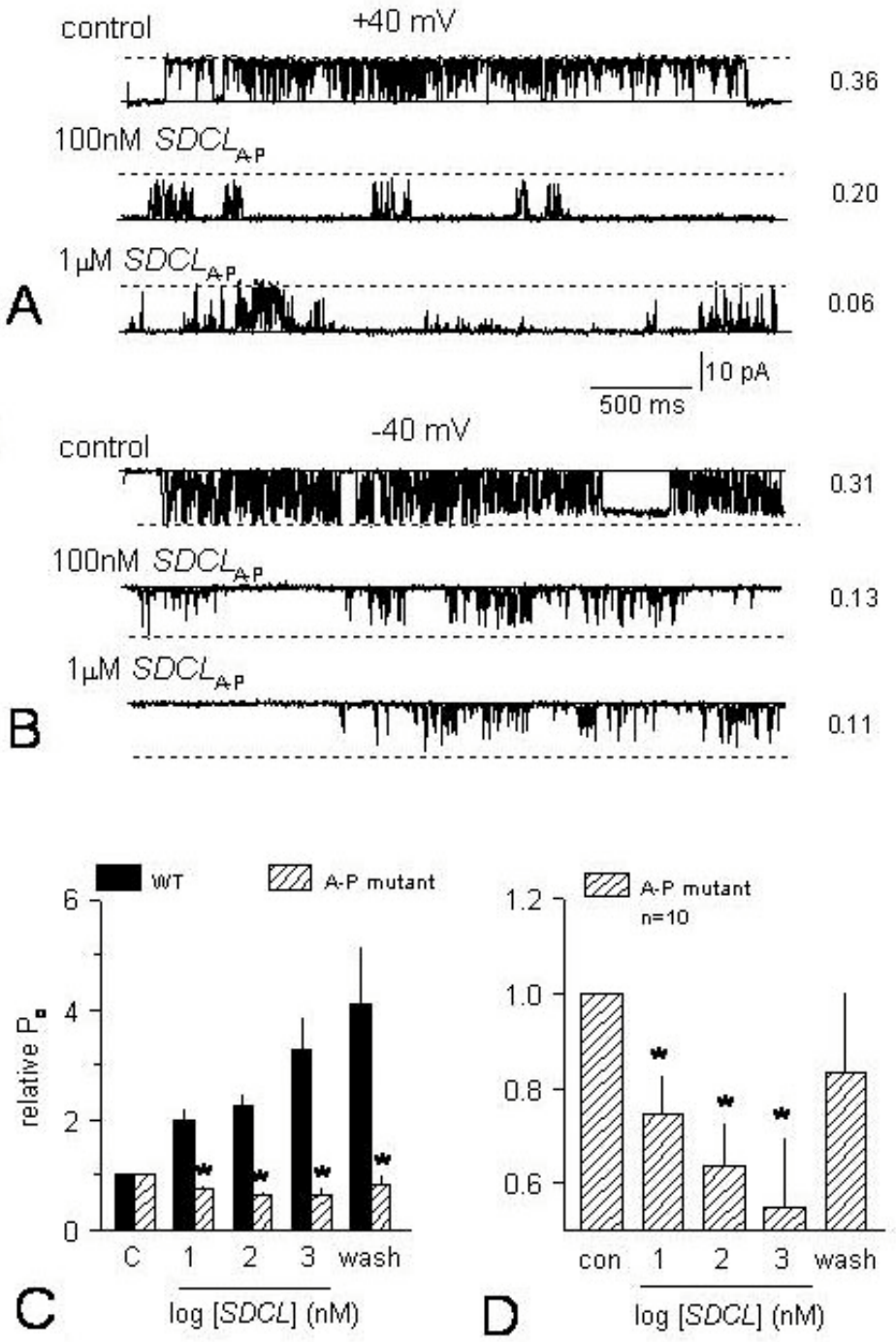

Figure 5. The single mutation in ***SDCL*$_{A\text{-}P}$** prevents the activation of native RyR1 channels by the recombinant loop, but does not prevent inhibition. (**A**) & (**B**) show 3 s current recordings from a single RyR1 channel at +40 and -40 mV respectively. The channel opens from the closed level (c, solid line) to the maximum single channel current (o, broken line). The 1st trace in each panel shows control data, the 2nd trace after adding 100 nM ***SDCL*$_{A\text{-}P}$** to the *cis* chamber and the 3rd trace after increasing the concentration to 1 microM. The numbers to the right of each trace show P_O for a 30 s recording under each condition. Channel activity decreases as the peptide concentration is increased at both potentials. (**C**) – comparison of average relative open probability (P_O) (combined +40 and -40 mV data) for 11 experiments with wild type ***SDCL*** (filled bins – data from figure 2 included for comparison) and 10 experiments with ***SDCL*$_{A\text{-}P}$** (hatched bins)**.** The relative P_O with the mutant loop is significantly less than that with the wild-type loop during exposure to ***SDCL*$_{A\text{-}P}$**. (**D**) – average relative P_O with ***SDCL*$_{A\text{-}P}$** (hatched bins) displayed with an expanded vertical axis to display inhibition by the mutant loop. The asterisks in (**C**) indicate significant differences between the wild-type and mutant data, while the asterisks in (**D**) indicate a significant decline from control with all ***SDCL*$_{A\text{-}P}$** concentrations.

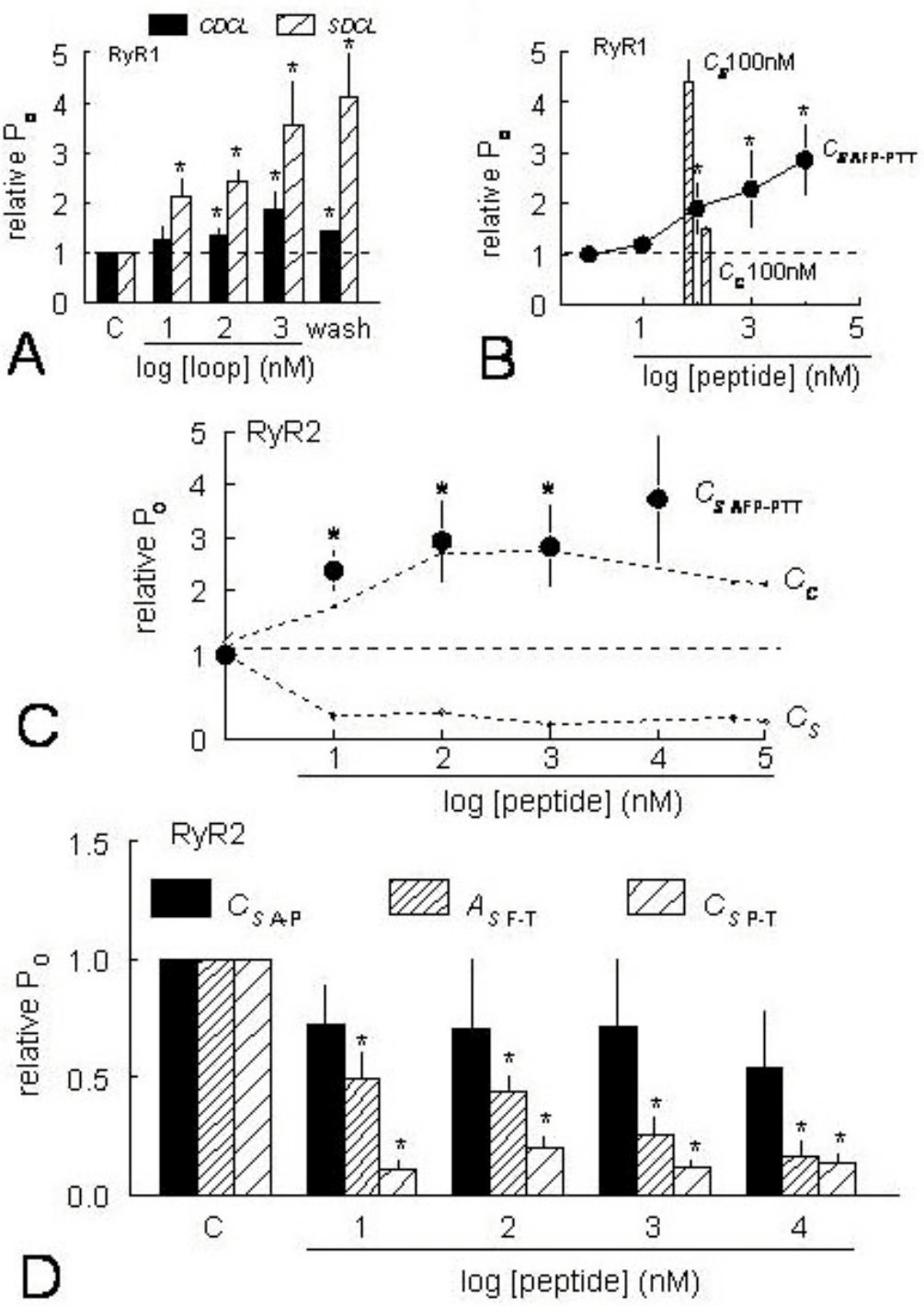

Figure 6. Activity of the wild type cardiac DHPR II-III loop (***CDCL***) and the mutant C_S peptides. Average relative open probability (P_O), shown as a function of loop (or peptide) concentration, includes data at +40 and -40 mV. (**A**) shows a comparison of the effects of ***CDCL*** (filled bins, N = 5 experiments) and ***SDCL*** (hatched bins, N = 11) on skeletal RyR1 channels. There is a significant increase in activity with ***CDCL***, but it is significantly less than that with ***SDCL***. (**B**) shows the effects of $C_{SAFP\text{-}PTT}$ on RyR1 (N = 5 experiments, filled circles). The data at 100 nM is compared with the effects of C_C (narrow-hatched bin) and C_S (wide-hatched bin) on RyR1 (21). (**C**) shows the effects of $C_{SAFP\text{-}PTT}$ on RyR2 (N = 6 experiments, filled circles). The data is compared with the effects of the wild type C_C (activation, upper broken line) and C_S (inhibition, lower broken line) on RyR2 from (6). (**D**) compares the effects of $C_{SA\text{-}P}$ (N = 5 experiments, filled bins), $C_{SF\text{-}T}$ (N = 5 experiments, narrow-hatched bins) and $C_{SP\text{-}T}$ (N = 4 experiments, wide-hatched bins) on RyR2 channels. The asterisks indicate significant differences between the control and test data.

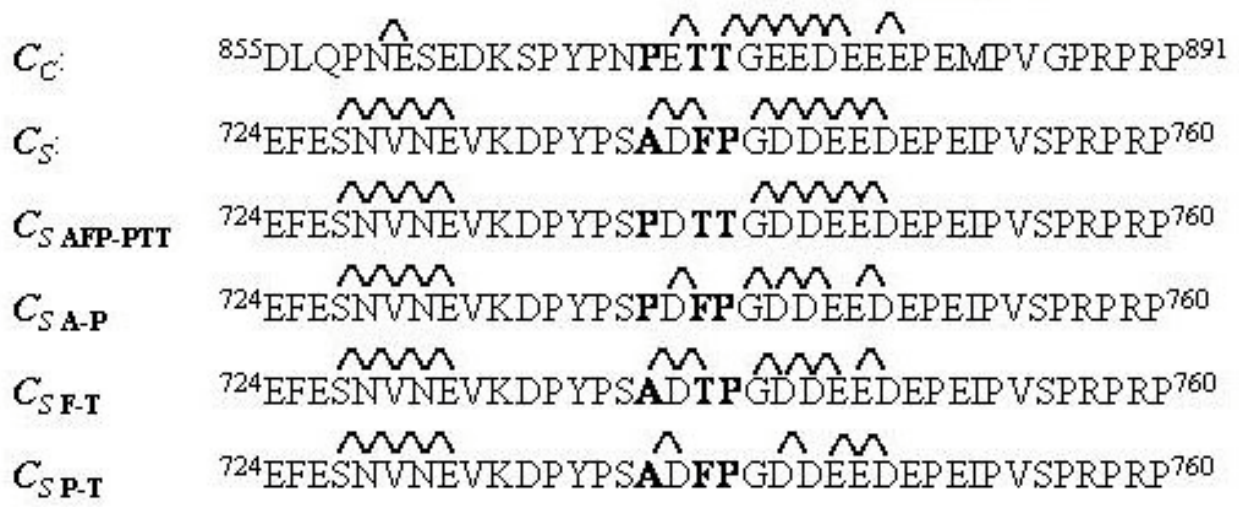

Figure 7. Results of the NMR NOE analysis of C_C, C_S and the four mutant C_S peptides. The ^ indicates NH-NH connectivities which are an indicator of helical structure between the adjacent residues. The assignment of residues have been determined by analysis of TOCSY and NOESY spectra obtained at 5° C. The secondary structure results for C_C and C_S have been published previously (6) and are included here for comparison. There is remarkably little difference in structure between any of the peptides.

4.5. Structure of the Mutant C_S peptides

We have previously shown with ^{1}H NMR that both the C_S and C_C peptides have the ability to form weak, partially structured alpha helices when examined at low temperatures (6). This evidence was obtained from the NH-NH connectivities in NOESY spectra which indicate that the residues are close in space and likely to adopt an alpha-helical structure. There are however minor structural differences between these peptides including a more structured N-terminal region for C_S and a marginally more extended alpha-helix toward the conserved clustered negatively charged region of C_C (figure 7 and (6)). The results of NMR analysis of the four mutant C_S peptides are also shown in figure 7. The triple AFP-PTT mutation reduced the nascent helix in the region of the mutated residues (consistent with P-TT being less helical than A-FP in the native cardiac and skeletal peptides respectively), but had no effect the helical nature of the downstream conserved negatively charged residues (figure 7). The A-P mutant is slightly less helical around the mutation site, as is the P-T mutant, when compared with wild type C_S. The secondary structure profile of the F-T mutant is not significantly different from the wild type C_S. No structural changes were observed between the N-terminal helical segment (SNVNE) in any of the mutants. It should be noted that various amino acids have different tendencies to form α-helices. Alanine has the greatest ability stabilise an alpha-helix, while proline (lacking an amide hydrogen) is least likely to do so (22). However, all NOE evidence points to a very weak helical structure in residues 739-742 in both the presence and absence of the prolines with the individual substitutions.

In an attempt to determine whether the mutations resulted in any gross conformational differences in ***SDCL***, we compared the chemical shift profile of the ^{15}N labelled wild type ***SDCL*** and $SDCL_{AFP\text{-}PPT}$ using ^{15}N/^{1}H spectra (not shown). NMR chemical shifts are dependent on the environment of the nuclei and are highly sensitive to structural and environmental perturbations. Apart from the mutated residues as well as their adjacent neighbours, only minor or no differences were observed in other regions including the cluster of negatively charged residues downstream from the mutations.

The conclusion from these mutation studies is that residue 739 is important in determining the functional activity of the skeletal II-III loop and ***C*** peptide, but none of residues 739-742 have a pronounced impact on the overall structural profile of the ***C*** region of the skeletal loop. We do not find any evidence for (i) individual mutations increasing the helical structure in the conserved cluster of negatively charge residues or (ii) that interactions with the RyR are reduced by helical content in the negatively charge residues.

5. DISCUSSION

This study provides the first molecular data on the consequences of mutations in the "***C***" region of the skeletal DHPR II-III loop on interactions between the II-III loop and the skeletal RyR and on the structure of the "***C***" region. The effects of substitution of cardiac residues for A739, F741 and P742 in the 126 residue skeletal DHPR II-III loop (***SDCL***) on its functional interactions with the skeletal muscle RyR1 have been examined. The structural and functional effects of the same mutations in a 37 residue skeletal "***C'***' region peptide, C_S are compared with the effects on the longer ***SDCL*** sequence. The mutations did not prevent interactions between the loop and the RyR, but the A-P substitution altered the functional consequences of the interactions. Novel observations were that (a) ***SDCL*** exerts high affinity activation and lower affinity inhibition on native RyR1 channels, (b) a single skeletal DHPR

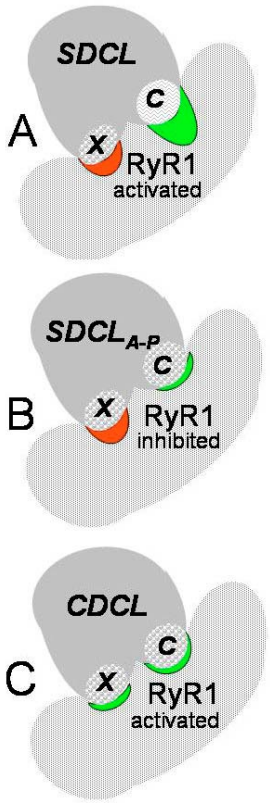

Figure 8. A model showing hypothetical interactions between the skeletal or cardiac DHPR II-III loop and RyR1. Interactions between the ***C*** region of ***SDCL*** and RyR1 strongly activate the channel (indicated by the green cone), while interactions between the ***C*** region in ***CDCL*** and RyR1 weakly activates the channel. A second region (***X***) in ***SDCL*** inhibits RyR1 (indicated by the red cone) or, in ***CDCL*** activates the channel. The channel is inhibited when inhibition is stronger than activation as with $\boldsymbol{SDCL_{A\text{-}P}}$.

residue, A739, is responsible for the excitatory action of the skeletal loop and its substitution for a proline rendered the loop inhibitory, (c) the mutations in peptide $\boldsymbol{C_S}$ also profoundly altered the ability of the peptide to activate RyRs and (d) the substitutions did not significantly alter the structure of the ***C*** residues. Although some of the altered interactions with RyR1 are consistent with changes in EC coupling following similar mutations in the DHPR in myocytes (9), the results suggest that changes in EC coupling may also depend on micro-targeting of DHPRs and RyRs since they do not abolish the interaction with the RyR or alter the secondary structure of the "***C***" residues.

5.1. Dual actions of both *SDCL* and *CDCL* on native skeletal RyRs

Both recombinant DHPR II-III loops bind to and activate purified RyR1, with ***CDCL*** being more active (10, 23). Both loops also bound to the native RyR1 with high affinity in the present study, although activation by ***CDCL*** was less than that by ***SDCL***. In addition to the high affinity slowly reversible activation, ***SDCL*** also induced a lower affinity rapidly reversible inhibition of the native RyR1. The A739P substitution in $\boldsymbol{SDCL_{AFP\text{-}PTT}}$ and $\boldsymbol{SDCL_{A\text{-}P}}$ prevented its activation of RyR1, but not its inhibitory effects. This selective removal of activation, and the different affinities and reversibility of activation and inhibition suggest that ***SDCL*** interacts with two separate sites on RyR1. The presence of two interaction sites is also suggested by the fact that the same substitutions in the 35 residue peptide $\boldsymbol{C_S}$ reduce its ability to activate RyR1, but did not render the peptide inhibitory. This effect on the ***C*** region could underlie the reduced activation by $\boldsymbol{SDCL_{AFP\text{-}PTT}}$ and $\boldsymbol{SDCL_{A\text{-}P}}$, but not the inhibitory action of these two mutant loops.

The observations can be reconciled by a model in which ***SDCL*** binds to RyR1 through two sites, inducing activation at one and inhibition at the other (figure 8). It is assumed that the ***C*** region binds to the activation site (see Discussion below). The substitutions in $\boldsymbol{SDCL_{AFP\text{-}PTT}}$ and $\boldsymbol{SDCL_{A\text{-}P}}$ reduce the loops activating ability by removing the alanine residue at position 739. The effect of the mutants on RyR activity is inhibitory because the interaction with the second site is retained**.** The hypothesis can be extended to include the actions of ***CDCL*** with the further assumptions (a) that activation of RyR1 by the ***C*** region in ***CDCL*** is less than activation by the ***C*** region in ***SDCL*** (because there is no alanine in the position equivalent to 739 in ***CDCL***) and (b) that the effect of the binding of the second region is to cause relatively weaker inhibition or weak activation. This final assumption is consistent with the reduced washout activation with ***CDCL***. This hypothesis reconciles the fact that the triple mutation in $\boldsymbol{C_{SAFP\text{-}PTT}}$ converts the function of the $\boldsymbol{C_S}$ peptide from skeletal-like to cardiac-like, but the same mutation in $\boldsymbol{SDCL_{AFP\text{-}PTT}}$ does not result in cardiac-like loop activity.

It is assumed that the loop interacts with the RyR through the ***C*** region because the isolated ***C*** residues modify channel activity (Introduction and Results), mutations in the ***C*** region alter interactions between the II-III loop and RyR1 (this study), and alter EC coupling (9). Competition studies suggest that the ***C*** region is also involved in ***CDCL*** binding to RyR2 (6). The second interaction site could be the ***A*** region (residues 671-690). Deletion and competition studies suggest that the ***A*** region in II-III loop interacts with RyR1 (6, 10, 23, 24). The high affinity interaction between RyR1 and peptide ***A*** activates the channel (Introduction) in contrast to the inhibitory effect postulated in the model outlined above. However ***A*** peptides have the potential to inhibit RyR1[1]. Activation of RyR1 by ***A*** and related peptides is reduced when *cis* $[Ca^{2+}]$ is >10 microM (unpublished and (25)), while the peptides inhibit RyR2 when *cis* $[Ca^{2+}]$ is activating (26). The effects on RyR2 are relevant because the actions of ***A*** and related peptides are not RyR isoform specific (26, 27) and responses of RyR2 are likely to reveal responses that could occur in RyR1.

5.2. Changes in the function of the C_S peptides were not correlated with structural changes

We have previously shown that there is little isoform specificity in the structure of the $\boldsymbol{C_C}$ and $\boldsymbol{C_S}$ (6).

Neither of the peptides had a strong alpha-helical structure such as that found in the ***A*** or the ***B*** regions (8, 16). Structural analysis in this study revealed only small differences between the structures of the wild type C_S and the mutant peptides. Weak nascent helices involving the ***C*** residues were in fact weaker in the $C_{SAFP\text{-}PTT}$ and $C_{SA\text{-}P}$ mutants whose actions most closely resembled C_C peptide (6). Thus the changes in activity were related to the A-P substitution rather than to any consistent change in helical content. The predicted increase in helical structure in the conserved negatively charged (DDEED) residues downstream from the ADFP sequence with 2 of the 3 individual mutations (9) was not seen in our structural analysis of either the ***C*** peptides or of ***SDCL***. There was a similar nascent helical structure in the DDEED region in the wildtype C_S and ***SDCL*** and in all mutants. The helical content in the DDEED residues was marginally less in $C_{SP\text{-}T}$ than in the other mutant peptides.

It is worth noting that our structural determinations with ***SDCL*** indicate that the structures of the ***A***, ***B*** and ***C*** regions in the full skeletal II-III loop are very similar to the structures of shorter peptides with sequences corresponding to each region (unpublished observations). It likely that the secondary structure will also be retained in the *in vivo* situation, even though the exact tertiary structure may vary. It is also likely that the secondary structures of the mutants determined here (figure 7) will be analogous to those in the wildtype peptide/protein. The results from this study indicate that there are no gross structural changes induced by the mutations in these peptide fragments which would affect the recognition of the RyR binding partner. However the amino acid substitution per se could affect recognition of the binding partner if the substituted amino acid was directly implicated in binding or the tertiary structure of the protein. An example of this was seen with the ***AB*** region of the II-III loop where the mutation of some residues resulted in a dramatic change in activity without altering the alpha helical secondary structure (8).

5.3. Comparison with whole cell studies

Individual A739P, F741T, P742T and D744E substitutions in the DHPR each disrupt skeletal EC coupling and it has been suggested that the residues are vital for an interaction with the RyR (9). Our results show that the A739P substitution alters, but does not prevent, the physical interaction between the RyR and either the full ***SDCL*** or ***C*** peptide. The individual F741T and P742T substitutions did not alter the effects of the II-III loop on the RyR. It is notable that the A739P mutation in whole cells altered EC coupling in a manner that was qualitatively different from that of the other mutations. Our results suggest that the F741T and P742T mutations must alter EC coupling in the whole cell by changing some parameter other than the ability of the DHPR and RyR to interact with each other. The mutations could, for example, alter the targeting of the proteins into positions that would allow them to physically interact. Such targeting could include the formation of tetrads or the precise alignment of tetrads with the RyR protein. Inappropriate targeting at this molecular level could well disrupt EC coupling but would not be detected with fluorescence microscopy. Another possibility that cannot be discounted is that the F741T and P742T mutations may alter the tertiary structure of the skeletal II-III loop in the *in vivo* situation in a manner that differs from the effects on the structure of the isolated ***SDCL***. The unavoidable conclusion from both our study and that of (9) is that interactions between the DHPR and RyR *in vivo* and *in vitro* are critically dependent on residues 739-742 in the skeletal sequence.

In summary, we show that introduction of a cardiac residue into position 739 of the skeletal DHPR II-III loop prevents the loop from activating the RyR in isolated systems. There is a strong correlation between the *in vitro* observation that residue 739 influences molecular interactions between the two proteins and *in vivo* measurements of EC coupling (9). The *in vitro* study of the ability of the two molecules to interact suggests that mutations in neighbouring residues 740-742 do not prevent a physical association between the ***C*** region and the RyR but may alter the micro-targeting of the DHPR and RyR in whole cells. In contrast to the changes in helical content that were predicted by (9), we find that there is no significant change in structure as a result of the mutations.

6. ACKNOWLEDGEMENTS

The authors are grateful to Suzy Pace and to Joan Stivala for assistance with preparation and characterisation of SR vesicles, to Sarah Watson for assistance with some of the single channel studies. We thank Professor Gerhard Meissner for providing us with cDNA for ***SDCL*** and ***CDCL***. The project was supported by a grant from the Australian National Health and Medical Research Council # 224235.

7. REFERENCES

1. Dulhunty, A. F., C. Haarmann, D. Green, D. R. Laver, P. G. Board and M. G. Casarotto: Interactions between dihydropyridine receptors and ryanodine receptors in striated muscle. *Prog Biophys Mol Biol* 79, 45-75 (2002)

2. Tanabe, T., K. G. Beam, J. A. Powell and S. Numa: Restoration of excitation-contraction coupling and slow calcium current in dysgenic muscle by dihydropyridine receptor complementary DNA. *Nature* 336, 134-139 (1988)

3. Wilkens, C. M., N. Kasielke, B. E. Flucher, K. G. Beam and M. Grabner: Excitation-contraction coupling is unaffected by drastic alteration of the sequence surrounding residues L720-L764 of the alpha 1S II-III loop. *Proc Natl Acad Sci USA* 98, 5892-7 (2001)

4. Ahern, C. A., D. Bhattacharya, L. Mortenson and R. Coronado: A component of excitation-contraction coupling triggered in the absence of the T671-L690 and L720-Q765 regions of the II-III loop of the dihydropyridine receptor alpha(1s) pore subunit. *Biophys J* 81, 3294-307 (2001)

5. Haarmann, C. C., D. Green, M. G. Casarotto, D. R. Laver and A. F. Dulhunty: The random coil C fragment of the DHPR II III loop can activate or inhibit native skeletal RyRs. *Biochem J* 372, 305-316 (2003)

6. Dulhunty, A. F., Y. Karunasekara, S. Curtis, P. J. Harvey, P. G. Board and M. G. Casarotto: The recombinant dihydropryidine receptor II-III loop and "*C*" region peptides modify cardiac ryanodine receptor activity. *Biochem J* in press, (2004)

7. Casarotto, M. G., F. Gibson, S. M. Pace, S. M. Curtis, M. Mulcair and A. F. Dulhunty: A structural requirement for activation of skeletal ryanodine receptors by peptides of the dihydropyridine receptor II-III loop. *J Biol Chem* 275, 11631-7 (2000)

8. Casarotto, M. G., D. Green, S. Pace, J. Young and A. F. Dulhunty: Activating the ryanodine receptor with dihydropyridine receptor fragments: size and charge do matter. *Front Biosc* 9, 2860-2872 (2004)

9. Kugler, G., R. G. Weiss, B. E. Flucher and M. Grabner: Structural requirements of the dihydropyridine receptor alpha1S II-III loop for skeletal-type excitation-contraction coupling. *J Biol Chem* 279, 4721-8 (2004)

10. Lu, X., L. Xu and G. Meissner: Activation of the skeletal muscle calcium release channel by a cytoplasmic loop of the dihydropyridine receptor. *J Biol Chem* 269, 6511-6 (1994)

11. Stange, M., A. Tripathy and G. Meissner: Two domains in dihydropyridine receptor activate the skeletal muscle Ca^{2+} release channel. *Biophys J* 81, 1419-29 (2001)

12. Yamamoto, T., J. Rodriguez and N. Ikemoto: Ca^{2+}-dependent dual functions of peptide C. The peptide corresponding to the Glu724-Pro760 region (the so-called determinant of excitation-contraction coupling) of the dihydropyridine receptor alpha 1 subunit II-III loop. *J Biol Chem* 277, 993-1001 (2002)

13. El-Hayek, R., B. Antoniu, J. Wang, S. L. Hamilton and N. Ikemoto: Identification of calcium release-triggering and blocking regions of the II-III loop of the skeletal muscle dihydropyridine receptor. *J Biol Chem* 270, 22116-22118 (1995)

14. Dulhunty, A. F., D. R. Laver, E. M. Gallant, M. G. Casarotto, S. M. Pace and S. Curtis: Activation and inhibition of skeletal RyR channels by a part of the skeletal DHPR II-III loop: effects of DHPR Ser687 and FKBP12. *Biophys J* 77, 189-203 (1999)

15. Gurrola, G. B., C. Arevalo, R. Sreekumar, A. J. Lokuta, J. W. Walker and H. H. Valdivia: Activation of ryanodine receptors by imperatoxin A and a peptide segment of the II-III loop of the dihydropyridine receptor. *J Biol Chem* 274, 7879-7886 (1999)

16. Casarotto, M. G., D. Green, S. M. Pace, S. M. Curtis and A. F. Dulhunty: Structural determinants for activation or inhibition of ryanodine receptors by basic residues in the dihydropyridine receptor II-III loop. *Biophys J* 80, 2715-26 (2001)

17. Catanzariti, A. M., T. A. Soboleva, D. A. Jans, P. G. Board and R. T. Baker: An efficient system for high-level expression and easy purification of authentic recombinant proteins. *Protein Sci* 13, 1331-9 (2004)

18. Porath, J. and B. Olin: Immobilized metal ion affinity adsorption and immobilized metal ion affinity chromatography of biomaterials. Serum protein affinities for gel-immobilized iron and nickel ions. *Biochemistry* 22, 1621-30 (1983)

19. Kay L. E., P. Keifer and T. Sarinen: Pure absorption gradient enhanced heteronuclear single quantum correlation spectroscopy with improved sensitivity. *J Am Chem Soc* 114, 10663-10665 (1992)

20. King, B. M., G. Bear: Some (almost) assumption-free tests. In: Statistical reasoning in psychology and education. Ed: E. W. Minium Wiley NY (1993)

21. Haarmann, C., A. F. Dulhunty and D. Laver: Regulation of skeletal ryanodine receptors by dihydropyridine receptor II-III loop C-region peptides: relief of Mg^{2+} inhibition. *Biochem J* (in press), (2005)

22. O'Neil, K. T. and W. F. DeGrado: A thermodynamic scale for the helix-forming tendencies of the commonly occurring amino acids. *Science* 250, 646-51 (1990)

23. Lu, X., L. Xu and G. Meissner: Phosphorylation of dihydropyridine receptor II-III loop peptide regulates skeletal muscle calcium release channel function. Evidence for an essential role of the beta-OH group of Ser687. *J Biol Chem* 270, 18459-64 (1995)

24. O'Reilly, F. M., M. Robert, I. Jona, C. Szegedi, M. Albrieux, S. Geib, M. De Waard, M. Villaz and M. Ronjat: FKBP12 modulation of the binding of the skeletal ryanodine receptor onto the II-III loop of the dihydropyridine receptor. *Biophys J* 82, 145-55 (2002)

25. Gallant, E. M., S. Curtis, S. M. Pace and A. F. Dulhunty: Arg(615)Cys substitution in pig skeletal ryanodine receptors increases activation of single channels by a segment of the skeletal DHPR II-III loop. *Biophys J* 80, 1769-82 (2001)

26. Dulhunty, A. F., S. M. Curtis, L. Cengia, M. Sakowska and M. G. Casarotto: Peptide fragments of the dihydropyridine receptor can modulate cardiac ryanodine receptor channel activity and sarcoplasmic reticulum Ca2+ release. *Biochem J* 379, 161-72 (2004)

27. Bannister, M. L., A. J. Williams and R. Sitsapesan: Removal of clustered positive charge from dihydropyridine receptor II-III loop peptide augments activation of ryanodine receptors. *Biochem Biophys Res Commun* 314, 667-74 (2004)

Footnote 1: Two types of inhibition are exerted by the ***A*** peptides. The one referred to here is seen with 10 – 100 nM peptide, is Ca^{2+} -dependent and voltage-independent (6). The other is a channel block seen only at +40 mV in symmetrical solutions and only with >1 microM peptide (1).

Key Words: Dihydropyridine receptor, Ryanodine receptor, Protein, protein interactions

Send correspondence to: Dr A F Dulhunty, PO Box 334, Canberra, ACT 2601, Australia, Tel: 61-2-6125-4491, Fax: 61-2-6125-4761, E-mail: angela.dulhunty@anu.edu.au

http://www.bioscience.org/current/vol10.htm